

Single electron capture in low- and intermediate-energy collisions of $Si^{3,4+}$ with He

Yingzhou Li(李英卓), Yadong Liu(刘亚东), Yueying Qi(祁月盈), Ling Liu(刘玲), Yizhi Qu(屈一至), and Jianguo Wang(王建国)

Citation: Chin. Phys. B, 2026, 35 (**1**): 013401. DOI: 10.1088/1674-1056/ae15f4
http://cpb.iphy.ac.cn; http://iopscience.iop.org/cpb

What follows is a list of articles you may be interested in

Experiment study of energy redistribution during collisions of the excited state $H_2(1, 7)$ with LiH

Kai Wang(王凯), Zhong Liu(刘中), Shuying Wang(王淑英), Chu Qin(秦楚), Zilei Yu(於子雷), and Xiaofang Zhao(赵小芳)

Chin. Phys. B, 2025, 34 (**11**): 113401. DOI: 10.1088/1674-1056/add502

Electron capture and excitation in intermediate-energy He^{2+}-H(1s,2s) collisions

Yadong Liu(刘亚东), Congcong Jia(贾聪聪), Mingxuan Ma(马茗萱), Xiang Gao(高翔), Ling Liu(刘玲), Yong Wu(吴勇), Xiangjun Chen(陈向军), and Jianguo Wang(王建国)

Chin. Phys. B, 2024, 33 (**8**): 083401. DOI: 10.1088/1674-1056/ad5322

Atomic structure and collision dynamics with highly charged ions

Xinwen Ma(马新文), Shaofeng Zhang(张少锋), Weiqiang Wen(汶伟强), Zhongkui Huang(黄忠魁), Zhimin Hu(胡智民), Dalong Guo(郭大龙), Junwen Gao(高俊文), Bennaceur Najjari, Shenyue Xu(许慎跃), Shuncheng Yan(闫顺成), Ke Yao(姚科), Ruitian Zhang(张瑞田), Yong Gao(高永), and Xiaolong Zhu(朱小龙)

Chin. Phys. B, 2022, 31 (**9**): 093401. DOI: 10.1088/1674-1056/ac8736

The influence of collision energy on magnetically tuned ^{6}Li-^{6}Li Feshbach resonance

Rong Zhang(张蓉), Yong-Chang Han(韩永昌), Shu-Lin Cong(丛书林), and Maksim B Shundalau

Chin. Phys. B, 2022, 31 (**6**): 063402. DOI: 10.1088/1674-1056/ac4cc3

Electron capture in collisions of Li^{3+} ions with ground andexcited states of Li atoms

M X Ma(马茗萱), B H Kou(寇博珩), L Liu(刘玲), Y Wu(吴勇), J G Wang(王建国)

Chin. Phys. B, 2020, 29 (**1**): 013401. DOI: 10.1088/1674-1056/ab577f

---

DATA PAPER

Single electron capture in low- and intermediate-energy collisions of $Si^{3,4+}$ with He

Yingzhou Li(李英卓)[1], Yadong Liu(刘亚东)[2,3], Yueying Qi(祁月盈)[4,†], Ling Liu(刘玲)[3,‡], Yizhi Qu(屈一至)[1], and Jianguo Wang(王建国)[3]

[1] *School of Optoelectronics, University of Chinese Academy of Sciences, Beijing* 100049, *China*
[2] *Hefei National Research Center for Physical Sciences at Microscale and Department of Modern Physics, University of Science and Technology of China, Hefei* 230026, *China*
[3] *Institute of Applied Physics and Computational Mathematitics, Beijing* 100088, *China*
[4] *College of Mechanical Engineering, Jiaxing University, Jiaxing* 314001, *China*

(Received 26 August 2025; revised manuscript received 12 October 2025; accepted manuscript online 22 October 2025)

The single electron capture processes in $Si^{3,4+}$+He collisions have been investigated theoretically employing the two-center atomic orbital close-coupling method in the energy range 0.01–100 keV/u. Total and state-selective electron capture cross sections for the dominant and subdominant reaction channels are calculated and compared with the available experimental and theoretical data. For the total charge transfer cross sections, the present results show better agreements with the available experimental data than the other theoretical ones in the overlapping energy region for both collision systems. For the state-selective cross sections, the present results for 3s and 3p states are in general agreement with the previous MOCC results in the low energy region for both collision systems. Furthermore, the cross sections for electron captured to the 3d, 4l and 5l ($l = 0, 1, \ldots, n-1$) states of Si^{2+} and Si^{3+} ions are first provided in a broad energy region in our work. These results are useful for the investigations in astrophysics. The datasets presented in this paper, including the total and state-selective electron capture cross sections of $Si^{3,4+}$+He collisions in 0.01–100 keV/u, are openly available at https://doi.org/10.57760/sciencedb.j00113.00257.

Keywords: atomic orbital close-coupling, single electron capture cross section

PACS: 34.50.–s, 34.10.+x

DOI: 10.1088/1674-1056/ae15f4 **CSTR:** 32038.14.CPB.ae15f4

1. Introduction

Charge transfer processes in ion–atom collisions have attracted considerable theoretical and experimental attention in the past decades due to their important role in laboratory plasmas and astrophysics. The astrophysical shock can be generated when the strong stellar wind[1,2] or the supernova explosion[3–5] passes through the planetary atmosphere or a nebula if their velocities exceed the sonic speed of the medium. After the shock wave passes through the medium, a vast amount of ionized gas (including H, He, O, N, Si[6,7]) can be obtained. If the velocity of the shock is high enough, the physical environment after the shock passing through can be conducive to the emission of various spectral lines.[8] In order to diagnose the ionization structure of the shocked interstellar gas, the accurate charge transfer cross sections for the collisions between the above ionized gas and H/He atoms[6,7] are needed. Moreover, the electron capture processes in astrophysical shocks have a substantial impact on the column densities, line intensities of the important ionic species like N, O, Si, and S in the astrophysical environment. Two theoretical models are proposed by Bulter *et al.*[6] to simulate the ionization structure of the interstellar gas after a shock impact. In the first model charge transfer processes are not taken into account, while the electron capture processes between all the important ionic species and neutral hydrogen and helium atoms are all included in the second model. By comparing the results from the above two models, they found charge transfer processes between ions and atoms play an important role in the simulations. When the shock travels at a speed of 120 km/s in the ionic gas, the proportion of Si^{4+} ions among all Si^{q+} ($q = 0, 1, 2, 3, 4$) ions is significantly reduced due to the charge transfer process of Si^{4+} with H or He in the temperature region $T \leq 2 \times 10^4$ K. Arun Mathew *et al.*[7] also considered that charge transfer reactions between C^{q+}, N^{q+}, O^{q+}, Ne^{q+}, Si^{q+}, S^{q+}, Fe^{q+} ($q = 1, 2, 3, 4$) ions and H/He atoms have an important effect on the ionization of gases. Therefore, the accurate charge transfer cross sections between ions and atoms and molecules are urgently needed.

The abundances of Si and He are very high in the supernova remnants, so the accurate investigation of the charge transfer processes between Si ions and He atoms is essential for the modeling of supernova remnants. In this paper, we

†Corresponding author. E-mail: yying_qi@mail.zjxu.edu.cn
‡Corresponding author. E-mail: liu_ling@iapcm.ac.cn

© 2026 Chinese Physical Society and IOP Publishing Ltd. All rights, including for text and data mining, AI training, and similar technologies, are reserved.

shall study the single electron capture processes for the collisions between $Si^{3,4+}$ ions and He atoms as

$$\begin{aligned} &Si^{4+}\left(1s^22s^22p^6\right)+He \\ \rightarrow\ &Si^{3+}\left(1s^22s^22p^6nl\right)+He^+, \end{aligned} \tag{1}$$

$$\begin{aligned} &Si^{3+}\left(1s^22s^22p^63s\right)+He \\ \rightarrow\ &Si^{2+}\left(1s^22s^22p^63snl\right)+He^+. \end{aligned} \tag{2}$$

The reports of electron capture cross sections for these systems are very scarce until now, especially for the state-selective charge transfer cross sections. Experimental total single- and double-electron capture cross sections for $Si^{3,4+}$–He collision systems have been measured by Tawara *et al.*[9] in the energy region 0.01–0.15 eV/u. To the best of our knowledge, the experimental data of *nl*-state-selective electron capture cross sections for these systems have not been reported so far.

On the theoretical side, the calculations of the single-electron capture process for Si^{4+}–He system have been performed in a number of studies, using various methods to describe the collision dynamics.

The semi-classical molecular orbital close-coupling (SMOCC) method was used by Opradolce *et al.*,[10] Bacchus-Montabonet *et al.*[11] and Suzuki *et al.*[12,13] to calculate the total and state-selective single-electron-capture cross sections in the energy region of 1.23×10^{-7}–5.0×1.0 keV/u, 6.4×10^{-4}–0.35 keV/u and 0.04–25 keV/u, respectively. Stancil *et al.*[14] employed a full quantum-mechanical molecular orbital close-coupling (QMOCC) method to calculate the total and state-selective cross sections over an energy range of 5.17×10^{-4}–0.2 keV/u. Vaeck *et al.*[15] performed calculations of total and state-selective cross sections by using a time-dependent wave-packet (TDWP) method in the energy range of 1.6×10^{-5}–0.25 keV/u. It is to be noted that only the state-selective cross sections for electron captured to the 3s and 3p states of Si^{3+} ions are reported for the low collision energies in the above mentioned theoretical studies.

For the Si^{3+}+He system, Honvault *et al.*[16] employed the *ab-initio* quantum mechanical methods to calculate the total and state-selective single-electron-capture cross sections within the collision energy range of 3.88×10^{-5}–0.25 keV/u. Stancil *et al.*[17] employed the MOCC method to calculate the total and state-selective cross sections for this system over a collision energy range of 2.93×10^{-7}–0.3 keV/u. Rabli *et al.*[18] employed a single-electron model potential to calculate the single-electron capture cross sections for the Si^{3+}+He system in energy ranging from 7.85×10^{-7} keV/u to 0.25 keV/u.

The main motivation of the present work is to investigate the electron capture dynamics for $Si^{3,4+}$–He collisions and provide reliable cross section data for single electron capture processes for these two systems in a broad energy region of 0.01–100 keV/u. The paper is organized as follows. In Section 2, a brief introduction of the theoretical method of the present work is given. The calculated cross sections are presented and discussed in Section 3. In Section 4, the conclusions are given. Atomic unit will be used throughout the paper unless otherwise noted.

2. Theoretical method

The two-center atomic orbital close-coupling (TC-AOCC) method has been described in detail elsewhere[19–22] to treat the collisions between ions and atoms in the low- and intermediate-energy regions. We briefly outline the main features of this method here. It is a semi-classical method in which the motion of nuclei follows a classical trajectory while the electronic dynamics is described by the quantum mechanical method. The relative projectile-target position $\boldsymbol{R}(t)$ is defined as $\boldsymbol{R}(t)=\boldsymbol{b}+\boldsymbol{v}t$, where $\boldsymbol{b}$ and $\boldsymbol{v}$ are the impact parameter and velocity, respectively. Under the impact parameter approximation, the time-dependent Schrödinger equation for the collision system can be written as

$$\left(H-\mathrm{i}\frac{\partial}{\partial t}\right)\varphi(\boldsymbol{r},t)=0, \tag{3}$$

where $H=-1/2\nabla_r^2+V_A(r_A)+V_B(r_B)$, V_A and V_B are the interactions between the active electron and the target and projectile, respectively. In the present calculations, one-active-electron model potentials are used to represent these interactions. For the $Si^{3,4+}$ ions, we have adopted the model potentials

$$V_{Si^{4+}}(r)=-\frac{4}{r}+\frac{1}{r}(-10-2.00272r)\,\mathrm{e}^{-3.76234r}, \tag{4}$$

$$V_{Si^{3+}}(r)=-\frac{3}{r}+\frac{1}{r}(-11-0.54294r)\,\mathrm{e}^{-2.60722r}. \tag{5}$$

For the He atoms, the one-electron model potential has the form

$$V_{He}(r)=-\frac{1}{r}+\frac{1}{r}(-1-0.65354r)\,\mathrm{e}^{-2.69697r}. \tag{6}$$

The binding energies of Si^{2+}, Si^{3+} ions and He atoms are calculated by the diagonalization of the single-center Hamiltonian with the above model potentials and compared with the corresponding data from the NIST table. From Table 1, we can see that our calculated binding energies for the $Si^{3+}(2p^6nl)$ ions show good agreement with the NIST data and the relative errors of the binding energies are less than 1%.

In Table 2, the binding energies for $Si^{2+}(2p^63snl)$ ion from Rabli *et al.*[18] are also given for comparison. They employed a model potential which includes eight independent parameters to describe the interaction between the active electron and Si^{3+} ions. From this table, we can see that our binding energies are in better agreement with the NIST data than the results obtained by Rabli *et al.*,[18] and the relative errors for this case are less than 5%.

Table 1. The calculated binding energies (a.u.) of $Si^{3+}(2p^6nl)$ ions compared with NIST data.[23]

nl	NIST	TC-AOCC (present work)	Error	nl	NIST	TC-AOCC (present work)	Error
3s	–1.659	–1.646	0.008	6s	–0.294	–0.293	0.003
3p	–1.333	–1.342	0.007	6p	–0.266	–0.267	0.004
3d	–0.928	–0.927	0.002	6d	–0.229	–0.229	3×10^{-4}
4s	–0.775	–0.773	0.007	6f	–0.223	–0.223	2×10^{-4}
4p	–0.664	–0.668	0.007	6g	–0.222	–0.222	4×10^{-4}
4d	–0.520	–0.520	4×10^{-4}	6h	–0.222	–0.222	1×10^{-4}
4f	–0.501	–0.501	0.001	7s	–0.207	–0.205	0.009
5s	–0.450	–0.449	0.002	7p	–0.190	–0.190	2×10^{-4}
5p	–0.399	–0.401	0.006	7d	–0.167	–0.167	0.001
5d	–0.331	–0.331	1×10^{-4}	7f	–0.164	–0.163	8×10^{-4}
5f	–0.321	–0.321	3×10^{-4}	7g	–0.163	–0.163	0.001
5g	–0.320	–0.320	3×10^{-4}	7h	–0.163	–0.163	0.001

Table 2. The calculated binding energies (a.u.) of $Si^{2+}(2p^63snl)$ ions compared with NIST data.[23]

nl	NIST	Rabli[18]	TC-AOCC (present work)	Error	nl	NIST	TC-AOCC (present work)	Error
3s	–1.231	–1.228	–1.231	0.001	6s	–0.184	–0.184	0.001
3p	–0.955	–0.851	–1.001	0.048	6p	–0.163	–0.168	0.033
3d	–0.554	–0.672	–0.552	0.003	6d	–0.136	–0.133	0.017
4s	–0.526	–0.505	–0.524	0.003	6f	–0.125	–0.125	0.005
4p	–0.431	–0.396	–0.451	0.047	6g	–0.126	–0.125	0.009
4d	–0.309	–0.333	–0.308	0.005	6h	–0.125	–0.125	0.002
4f	–0.281		–0.282	0.002	7s	–0.127	–0.126	0.008
5s	–0.290		–0.290	0.001	7p	–0.115	–0.118	0.025
5p	–0.252		–0.259	0.028	7d	–0.094	–0.097	0.032
5d	–0.196		–0.194	0.007	7f	–0.092	–0.091	0.008
5f	–0.187		–0.181	0.035	7g	–0.093	–0.091	0.014
5g	–0.182		–0.180	0.008	7h	–0.092	–0.092	0.006

The total wave function of the collision system can be written as

$$\varphi(\boldsymbol{r},t)=\sum_i c_i(t)\,\phi_i^A(\boldsymbol{r},t)+\sum_j d_j(t)\,\phi_j^B(\boldsymbol{r},t), \tag{7}$$

where ϕ_i^A and ϕ_j^B are the atomic states centered on $Si^{3,4+}$ ions and He atoms, respectively. These atomic states can be described by the even-tempered Slater-type orbital (STO) as

$$\phi_{nlm}(\boldsymbol{r})=\sum_k \tilde{c}_{nk}\chi_{klm}(\boldsymbol{r}) \tag{8}$$

with

$$\begin{aligned}&\chi_{klm}(\boldsymbol{r})=N_l(\xi_k)\,r^l\,\mathrm{e}^{-\xi_k r}\mathrm{Y}_{lm}(\hat{\boldsymbol{r}}),\\&\xi_k=\alpha\beta^k,\quad k=1,2,\ldots,N,\end{aligned} \tag{9}$$

where $N_l(\xi_k)$ is the normalization constant, $\mathrm{Y}_{lm}(\hat{\boldsymbol{r}})$ are the spherical harmonics, and α and β are variational parameters that can be determined by using the variational method to reproduce the one-electron binding energies. The expansion coefficient $\tilde{c}_{nk}$ can be obtained by diagonalizing the single-center Hamiltonian. The scattering amplitudes $c_i(t)$ and $d_j(t)$ can be obtained by solving the following coupled differential equations:

$$\mathrm{i}\left(\dot{C}+S\dot{D}\right)=HC+KD,\quad \mathrm{i}\left(\dot{D}+S^{\dagger}\dot{C}\right)=\bar{K}C+\bar{H}D, \tag{10}$$

where C and D are the scattering amplitude vectors of c_i $(i=1,2,\ldots)$ and d_j $(j=1,2,\ldots)$, respectively. S, H, $\bar{H}$, K and $\bar{K}$ are matrix elements. Under the initial conditions $d_{nlm}(-\infty)=\delta_{n,1}\delta_{l,0}\delta_{m,0}$, $c_{nlm}(-\infty)=0$, the nl-state-selective cross sections of electron capture process can be obtained by

$$\sigma_{nlm}^{cx}=2\pi\int_0^{\infty}|c_{nlm}(+\infty)|^2\,b\,\mathrm{d}b. \tag{11}$$

For the total electron capture cross sections, they can be obtained by the summation of all the partial cross sections as

$$\sigma_{\mathrm{total}}^{cx}=\sum_{nlm}\sigma_{nlm}^{cx}. \tag{12}$$

3. Results and discussion

3.1. Si^{4+}–He collisions

In the present TC-AOCC calculations, we have used an expansion basis containing all the states with $n\le 8$ ($l\le 5$) (in total 30 states) centered on $Si^{3+}(2p^6nl)$ and $Si^{2+}(2p^63snl)$ ions, and all the states with $n\le 4$ ($l\le 3$) (in total 10 states) centered on He atoms. In order to check the convergence of this basis, we have used basis sets with different sizes on the projectile for different collision energies to calculate the cross sections. The total and dominant partial cross sections for electron capture process in Si^{4+}–He and Si^{3+}–He collision systems with different expansion basis sets are shown in Tables 3 and 4, respectively. It can be seen that with the present basis the convergence of the results is achieved for different energy regions.

Table 3. Total and $3l$-state-selective single-electron-capture cross sections (in units of 10^{-16} cm^2) for Si^{4+}–He collisions with different sizes of expansion basis sets at the energies of 1 keV/u, 10 keV/u and 100 keV/u.

E (keV/u)	State	Si^{3+} ($n \leq 6$)/He ($n \leq 4$)	Si^{3+} ($n \leq 7$)/He ($n \leq 4$)	Si^{3+} ($n \leq 8$)/He ($n \leq 4$)
1	total	12.73553	13.04830	13.10066
	3s	9.08104	9.19132	9.09808
	3p	3.14053	3.20779	3.17918
	3d	0.13020	0.12290	0.14185
10	total	8.74537	8.87520	8.91642
	3s	4.71375	4.75024	4.72897
	3p	3.11772	3.11368	3.11691
	3d	0.51590	0.51726	0.51510
100	total	2.07695	2.23071	2.23071
	3s	0.08952	0.08910	0.08910
	3p	0.37904	0.37770	0.37770
	3d	0.62531	0.63073	0.63073

Table 4. Total and $3l$-state-selective single-electron-capture cross sections (in units of 10^{-16} cm^2) of Si^{3+}–He collisions with different sizes of expansion basis sets at the energies of 1 keV/u, 10 keV/u and 100 keV/u.

E (keV/u)	State	Si^{2+} ($n \leq 6$)/He ($n \leq 4$)	Si^{2+} ($n \leq 7$)/He ($n \leq 4$)	Si^{2+} ($n \leq 8$)/He ($n \leq 4$)
1	total	5.97279	5.77305	6.03626
	3s	5.31919	5.20711	5.28067
	3p	0.27302	0.30594	0.28358
	3d	0.15153	0.17201	0.16803
10	total	5.81019	5.74824	5.69412
	3s	3.62577	3.48010	3.38618
	3p	1.55552	1.58884	1.58953
	3d	0.31183	0.29524	0.27971
100	total	1.26608	1.31368	1.34298
	3s	0.07905	0.07879	0.07873
	3p	0.36094	0.36088	0.36060
	3d	0.27077	0.27100	0.27133

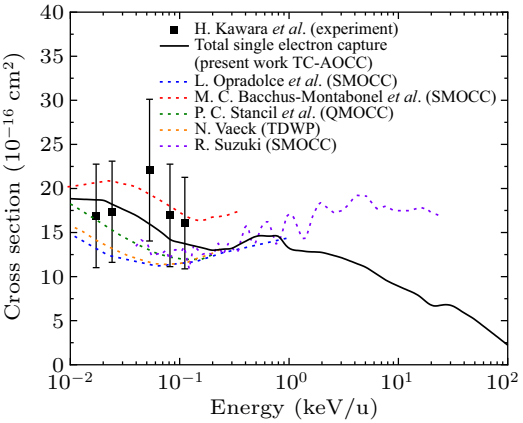


Fig. 1. Total cross sections for single electron capture process in Si^{4+}–He collisions. The squares represent the experimental data of Ref. [9], the black solid lines represent present TC-AOCC work, the blue dashed lines represent the SMOCC results of Ref. [10], the red dashed lines represent the SMOCC results of Ref. [11], the green dashed lines represent the QMOCC results of Ref. [14], the yellow dashed lines represent the TDWP results of Ref. [15] and the purple dashed lines represent the SMOCC results of Refs. [12,13].

The present total single-electron-capture cross sections for the Si^{4+}–He system are shown in Fig. 1. The previous theoretical and experimental data are also given in the same figure for comparison. From this figure, we can see that the present TC-AOCC results are in general agreement with the experimental data of Tawara *et al.*[9] in the energy region below about 0.15 keV/u. Above this energy, the present results increase with increasing collision energy and then decrease. We note that the present results have the same energy behavior with the SMOCC results of Opradolce *et al.*,[10] QMOCC results of Stancil *et al.*[14] and time-dependent wave packet (TDWP) method results of Vaeck *et al.*[15] in the same energy region, but the magnitudes of our results are a little larger than these theoretical results. The discrepancies between our results and those of other theoretical methods may come from the different numbers of reaction channels and the model potentials that were used in the cross-section calculations. The SMOCC results of Bacchus-Montabonel *et al.*[11] are obviously larger than the other theoretical results in the energy region below 0.15 keV/u, and the energy behavior of their cross sections is also different from that of the other theoretical results. It is to be noted that the SMOCC results of Suzuki *et al.*[12,13] exhibit obviously oscillatory structures in the energy region above 0.04 keV/u, and the values of their results are in good agreement with our TC-AOCC results in the energy region 0.04–1.0 keV/u. The two-state approximation which was proposed by Smith *et al.*[24] was used in their calculations and they considered that these structures were mainly from the oscillations in the dominant state-selective cross sections of $Si^{3+}(2p^6 3s)$ state. But for the energies above 1.0 eV/u, the SMOCC results of Suzuki *et al.*[12,13] are significantly larger

than our results. Only 3s, 3p, 3d and 4s states of ion $Si^{3+}(nl)$ were considered in the calculation of Suzuki *et al.*[12,13] However, the high excited states of Si^{3+} ions will have big contributions to the total single-electron-capture cross sections for the high collision energies.

In Fig. 2 we show our n-resolved electron-capture cross sections for the Si^{4+}–He collision system. From this figure, we can see that $n = 3$ is the dominant reaction channel for this collision system in the whole energy region and the magnitudes for the $n = 3$ cross sections are significantly larger than those captured into the $n = 4$ and $n = 5$ channels.

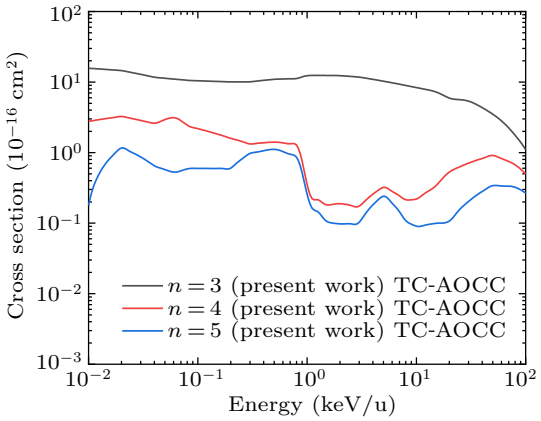


Fig. 2. The n-resolved single-electron-capture cross sections for Si^{4+}–He collisions.

The nl-state-selective electron-capture cross sections for the Si^{4+}–He system are displayed in Fig. 3, together with the QMOCC results of Stancil *et al.*,[14] the SMOCC results of Opradolce *et al.*,[10] Bacchus-Montabonel *et al.*[11] and Suzuki *et al.*,[12,13] the TDWP results of Vaeck *et al.*[15] For this collision system, $3l$ states of Si^{3+} ions are the dominant reaction channels in the whole energy region. From Fig. 3(a) we can see that below 0.1 keV/u, the 3p state of Si^{3+} ions is the dominant channel in the present calculations. With the increase of collision energy, the 3s state becomes the dominant one in the energy region 0.1–15 keV/u. We can see that the present 3s and 3p capture cross sections have the same energy behavior as those of other theoretical methods, but the magnitudes are different in the overlapping energy region. Above 15 keV/u, the 3p state becomes the dominant channel again. For the 3d states, only Suzuki *et al.*[12,13] included it in their cross section calculations. It can be seen that the present 3d cross sections have different magnitudes and energy behavior from those of Suzuki *et al.*[12,13] in the overlapping energy region, except for $E = 0.2$–0.4 keV/u. The differences between present $3l$ capture cross sections and the SMOCC results of Suzuki *et al.*[12,13] are mainly from the different numbers of reaction channels included in the cross section calculations. For the sub-dominant reaction channels $4l$ and $5l$ states, we can see from Figs. 3(b) and 3(c) that these cross sections are significantly smaller than the $3l$ captured cross

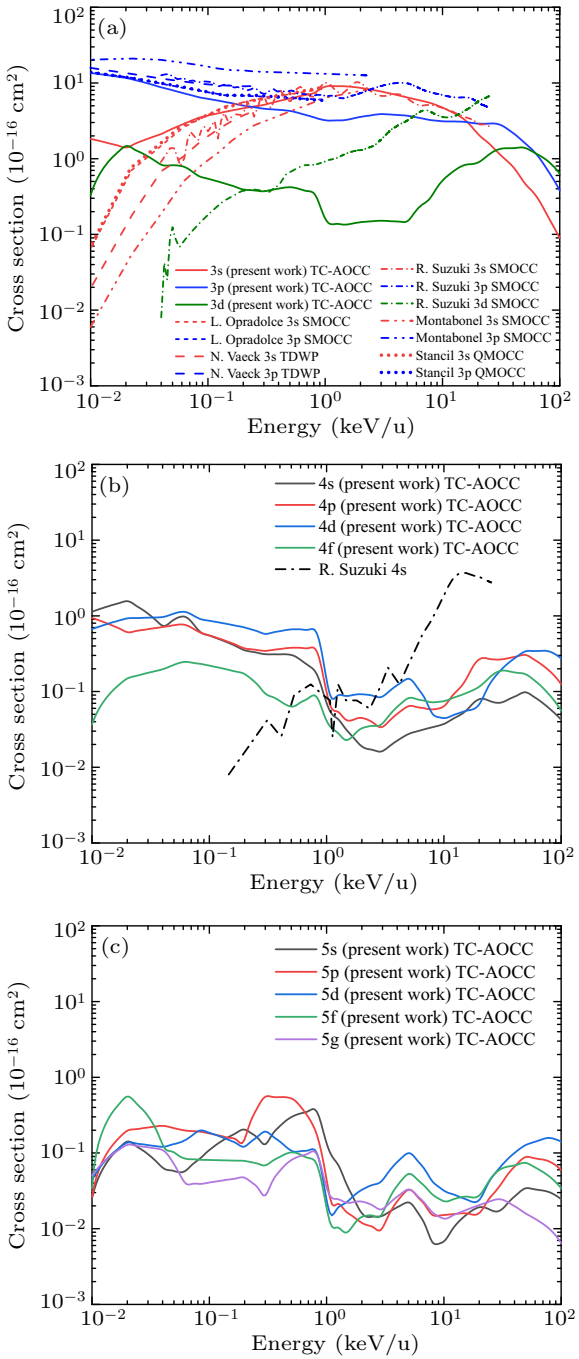


Fig. 3. The nl-state-selective cross sections of single electron capture in Si^{4+}–He collisions. (a) The full solid lines represent present TC-AOCC work; the short dashed lines represent the SMOCC results of Ref. [10]; the long dashed lines represent TDWP results of Ref. [15]; the dotted dashed lines represent the SMOCC results of Refs. [12,13]; the double-dots dash lines represent the SMOCC results of Ref. [11]; the dotted lines represent the QMOCC results of Ref. [14]. (b) This work (full lines), Refs. [12,13] (dotted dashed lines). (c) This work (full lines).

sections in the considered energy region. For the $4l$ reaction channels, only 4s cross sections are reported in the calculations of Suzuki *et al.*,[12,13] but their results are significantly larger than those of our TC-AOCC method in the whole energy range. The reason for the difference between our results and those of Suzuki *et al.*[12,13] has been mentioned above. Moreover, it can be seen that the $4l$ and $5l$ captured cross sections exhibit obviously oscillatory structures in the whole energy re-

gion. The more complex population dynamics of the $4l$ and $5l$ states results in the oscillatory structures in their capture cross sections in the energy region below about 50 keV/u.

3.2. Si^{3+}–He collisions

The total single-electron-capture cross sections for the Si^{3+}–He system are shown as a function of collision energy in Fig. 4. The other available theoretical and experimental data are also given in this figure for comparison. We can see that the present TC-AOCC results are in better agreement with the experimental data of Tawara *et al.*[9] than the other theoretical results in the energy region 0.01–0.10 keV/u. It is to be noted that the *ab-initio* results of Honvault *et al.*[16] and the results of Rabli *et al.*[18] are obviously lower than the present results and the MOCC results of Stancil *et al.*[17] in the overlapping energy region. Within the collision energy range of 0.1–0.2 keV/u, the present results agree with the MOCC results of Stancil *et al.*[17] However, at the collision energy of 0.04 keV/u, our results are significantly higher than the MOCC result of Stancil *et al.*[17] This discrepancy may be due to a fact that the $n \geq 4$ states of Si^{2+} ions are not included in the calculation of Stancil *et al.*[17] Table 5 shows the results of n-resolved state-selective cross-sections in the energy range of 0.01–100 keV/u. It can be observed that in the energy range of $E < 0.1$ keV/u, the state-selective cross sections for the $n = 3$ state are approximately three times larger than those of the $n \geq 4$ states. This means that in the energy region of $E < 0.1$ keV/u, the state-selective cross sections from the $n \geq 4$ states cannot be ignored.

Figure 5 shows the n-resolved electron capture cross sections for the Si^{3+}–He system. As shown in this figure and Table 5, although $n = 3$ is the dominant reaction channel for this collision system in the whole energy region, the ratios of the $n \geq 4$ capture cross sections to those of $n = 3$ state are different in different energy regions.

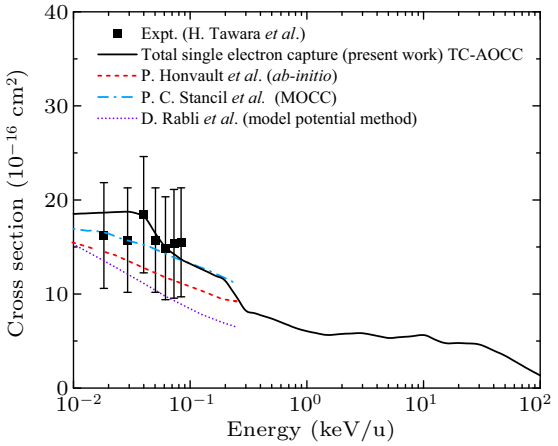


Fig. 4. Total cross sections of single electron capture process in Si^{3+}–He collisions. The squares represent the experimental data of Ref. [9], the black solid lines represent present TC-AOCC work, the blue dotted dashed lines represent the MOCC results of Ref. [17], the red dashed lines represent the results obtained by *ab-initio* method from Ref. [16], the purple dotted lines represent the results obtained by model potential method from Ref. [18].

Table 5. The n-resolved state-selective cross sections in the energy range of 0.01–100 keV/u.

Energy (keV/u)	Cross section (10^{-16} cm^2)		
	$n = 3$	$n = 4$	$n = 5$
0.01	10.16781	1.83251	1.49581
0.03	10.18558	1.49447	0.86376
0.04	10.42538	2.12846	1.08974
0.06	9.95049	1.70783	0.54484
0.085	9.00655	1.82948	0.64338
0.2	8.45281	1.03971	0.46580
0.3	7.16558	0.30731	0.20869
0.5	6.49058	0.28904	0.22818
0.8	6.03407	0.13699	0.07550
1	5.73228	0.13063	0.06278
1.5	5.31092	0.12333	0.05979
2	5.16927	0.27279	0.16686
3	5.18607	0.30818	0.20060
5	5.09106	0.11077	0.04610
8	5.14680	0.11958	0.05433
10	5.25542	0.17600	0.07242
15	4.33666	0.22050	0.05992
20	4.28416	0.25565	0.06908
30	3.69201	0.45285	0.15259
50	2.42632	0.53793	0.20304
80	1.14148	0.38388	0.18252
100	0.71066	0.27758	0.14245

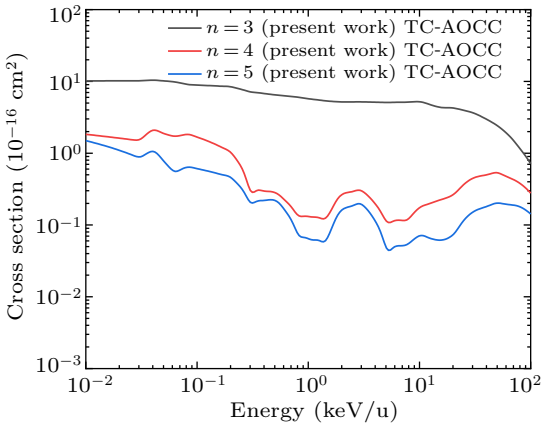


Fig. 5. The n-resolved single-electron-capture cross sections for Si^{3+}–He collisions.

The nl-state-selective single-electron-capture cross sections for Si^{3+}–He system are displayed in Fig. 6, together with the MOCC results of Stancil *et al.*,[17] the *ab-initio* results of Honvault *et al.*[16] For this collision system, the $n = 3$ state of Si^{2+} ion is the dominant reaction channel in the whole energy region. Compared with Fig. 3(a), we can see that the 3s state is the dominant charge transfer channel in the energy below 0.3 keV/u for the Si^{3+}–He collisions system. This is due to the fact that the channel $Si^{2+}(2p^6 3s^2)+He^+(1s)$ exhibits the strongest coupling with the initial channel $Si^{3+}(2p^6 3s)+He(1s^2)$ at the large internuclear distances. The present 3s and 3p capture cross sections are in general agreement with the other theoretical results in the overlapping energy region. It can also be seen that the

present 3p state of Si^{2+} ion becomes the dominant reaction channel for the collision energies above 17 keV/u. No 3d capture cross sections are reported for this system in the above mentioned theoretical calculations. From Fig. 6(a) we can see that the present 3d cross sections are larger than that of 3p state in the energy region below about 0.3 keV/u, and with the increasing collision energy, the magnitudes of 3d capture cross sections become smaller that of 3p state. The 4*l* and 5*l* states collision system, and the magnitudes of these states are significantly smaller than those of 3*l* states in the whole energy region. It is worth noting from Figs. 6(b) and 6(c) that the present 4*l* and 5*l* capture cross sections exhibit some oscillatory structures in the considered energy region.

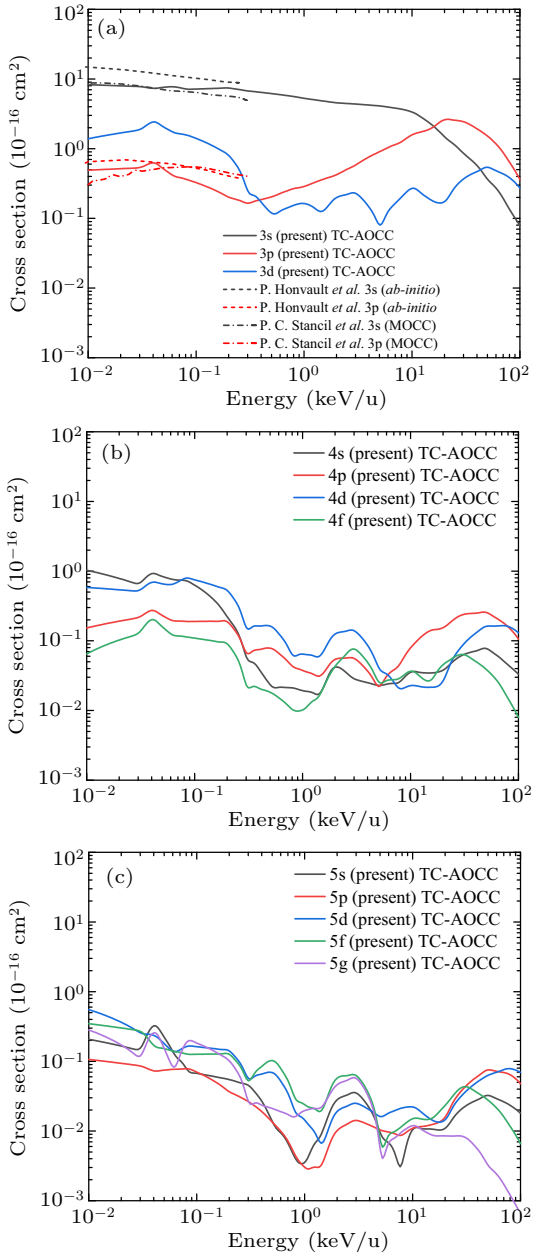


Fig. 6. The *nl*-state-selective cross sections of single electron capture in Si^{3+}–He collisions. The full solid lines represent present TC-AOCC work; the short dashed lines represent the results obtained by *ab-initio* method from Ref. [16]; the dotted dashed lines represent the MOCC results of Ref. [17].

4. Conclusion

In the present work, we have performed calculations for the total, *n*-resolved and *nl*-state-selective electron capture cross sections for $Si^{3,4+}$–He collision systems by using the semi-classical TC-AOCC method over an energy range of 0.01–100 keV/u. For the total electron capture cross sections, good agreements between the present results and the experimental data are obtained for both collision systems in the overlapping energy region. For the *nl*-state-selective cross sections, the present 3s and 3p captured cross sections of the Si^{4+}–He and Si^{3+}–He systems are both in good agreement with the previous MOCC results[14,17] within the overlapping energy range. Our 3d cross sections for Si^{4+}–He collisions are significantly different from the SMOCC results of Suzuki *et al.*[12,13] in the overlapping energy region. The *n*-resolved, 4*l*- and 5*l*-state-selective single charge transfer cross sections are first provided for these two collision systems. The 4*l* and 5*l* captured cross sections exhibit some oscillatory structures in the considered energy region due to their more complex population dynamics. These cross section data are useful for the simulation and modeling of the x-ray emission in different astrophysical environments.

Data availability statement

All the datasets presented in this paper, including the the total and state-selective electron capture cross sections of $Si^{3,4+}$+He collisions in 0.01–100 keV/u, are compiled in the supplementary materials (SM) in PDF format. The data that support the findings of this study are openly available in Science Data Bank via the link https://doi.org/10.57760/sciencedb.j00113.00257.

Acknowledgements

This work was supported by the National Key Research and Development Program of China (Grant No. 2022YFA1602504) and the National Natural Science Foundation of China (Grant Nos. 12274040 and U2430208).

References

[1] Granot A, Nakar E and Levinson A 2018 *Monthly Notices of the Royal Astronomical Society* **476** 5453
[2] Antokhin I I, Owocki S P and Brown J C 2004 *The Astrophysical Journal* **611** 434
[3] Vink J 2020 *Physics and evolution of supernova remnants* (Switzerland AG: Springer) p. 55
[4] Reynolds S P 2008 *Annu. Rev. Astron. Astrophys.* **46** 89
[5] Ellison D C, Reynolds S P and Borkowski K, *et al.* 1994 *Publications of the Astronomical Society of the Pacific* **106** 780
[6] Butler S E and Raymond J C 1980 *Astrophysical Journal* **240** 680
[7] Mathew A, Mackey J, Celeste M, *et al.* 2025 *Astronomy & Astrophysics* **695** A73
[8] Michael E, Zhekov S, McCray R, *et al.* 2002 *The Astrophysical Journal* **574** 166
[9] Tawara H, Okuno K, Fehrenbach C W, *et al.* 2001 *Phys. Rev. A* **63** 062701

[10] Opradolce L, McCarroll R and Valiron P 1985 *Astronomy and Astrophysics* **148** 229

[11] Bacchus-Montabonel M C and Ceyzeriat P 1998 *Phys. Rev. A* **58** 1162

[12] Suzuki R, Watanabe A, Sato H, *et al.* 2001 *Phys. Rev. A* **63** 042717

[13] Suzuki R, Watanabe A, Sato H, Gu J P, Hirsch G, Buenker R J, Kimura M and Stancil P C 2001 *Phys. Scr.* **T92** 345

[14] Stancil P C, Zygelman B, Clarke N J and Cooper D L 1997 *Phys. Rev. A* **55** 1064

[15] Vaeck N, Bacchus-Montabonel M C, Baloïtcha E and Desouter-Lecomte M 2001 *Phys. Rev. A* **63** 042704

[16] Honvault P, Bacchus-Montabonel M C, Gargaud M and McCarroll R 1998 *Chem. Phys.* **238** 401

[17] Stancil P C, Clarke N J, Zygelman B and Cooper D L 1999 *J. Phys. B: atom. Mol. Opt. Phys.* **32** 1523

[18] Rabli D, Gargaud M and McCarroll R 2001 *J. Phys. B: atom. Mol. Opt. Phys.* **34** 1395

[19] Ma M X, Kou B H, Liu L, Wu Y and Wang J G 2020 *Chin. Phys. B* **29** 013401

[20] Liu Y D, Lia C C, Ma M X, Gao X, Liu L, Wu Y, Chen X J and Wang J G 2024 *Chin. Phys. B* **33** 083401

[21] Bransden B H and McDowell M R C 1992 *Charge Exchange and the Theory of Ion–Atom Collisions* (Oxford: Clarendon Press) p. 152

[22] Fritsch W and Lin C D 1991 *Physics Reports* **202** 1

[23] http://physics.nist.gov/PhysRefData/ASD/index.html

[24] Smith F J 1966 *Phys. Lett.* **20** 271